Environmental Science & Technology

Article

Cite This: Environ. Sci. Technol. 2019, 53, 127−136

pubs.acs.org/est

Photochemical Aging of Guaiacol by Fe(III)−Oxalate Complexes in Atmospheric Aqueous Phase

Hongwei Pang,[†] Qi Zhang,[‡] Hongli Wang,[§] Dongmei Cai,[†] Yingge Ma,[§] Li Li,[§] Kangning Li,[†] Xiaohui Lu,*[,†] Hong Chen,[†] Xin Yang,*[,†,∥] and Jianmin Chen[†]

[†]Shanghai Key Laboratory of Atmospheric Particle Pollution and Prevention, Department of Environmental Science and Engineering, Fudan University, Shanghai 200433, China

[‡]Department of Environmental Toxicology, University of California, Davis, California 95616, United States

[§]State Environmental Protection Key Laboratory of Formation and Prevention of the Urban Air Pollution Complex, Shanghai Academy of Environmental Sciences, Shanghai 200233, China

[∥]Shanghai Institute of Pollution Control and Ecological Security, Shanghai 200092, China

Supporting Information

ABSTRACT: Fe(III)−oxalate complexes are likely abundant in clouds, fogs and aerosol water. They are photoreactive and can act as an important source of reactive oxygen species (·OH, H_2O_2 and HO_2·) in tropospheric aqueous phases. Although the mechanisms involved in ferrioxalate photolysis have been investigated extensively, few kinetic and mechanistic information is available on the aging of dissolved organic compounds by this photochemical system. In this work, the Fe(III)−oxalate mediated photooxidation of guaiacol (GUA), a model for phenolic compounds emitted from biomass burning, was investigated under typical pH conditions of the atmospheric water. The effect of Fe(III) concentration, oxalate concentration and pH on the photooxidation of GUA was studied in detail. Our results revealed that oxalate can inhibit the oxidation of GUA by Fe(III) under the dark condition. However, the iron-catalyzed photooxidation of GUA can be strongly promoted in the presence of oxalate due to the formation of photoactive Fe(III)−oxalate complexes. GUA was rapidly oxidized to form a number of polymeric, functionalized and open-ring products with low volatility. Detailed reaction pathways for the photooxidation of GUA by Fe(III)−oxalate complexes were proposed based on the results of high-resolution mass spectrometry. This work suggests that ferrioxalate photochemistry can play an important role in the transformation of dissolved organics in atmospheric aqueous phases.

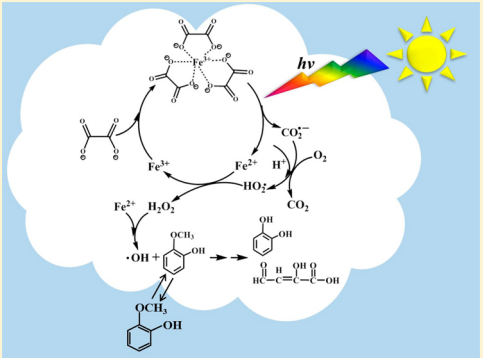

1. INTRODUCTION

Transition metals play an important role in the aging and transformation of inorganic and organic contents in atmospheric liquid phase.[1,2] Iron, the most abundant transition metal in the Earth's crust, has been identified as an important component in cloud and fog droplets.[1,3] The concentration of iron can range from micromolar to millimolar in cloud droplets and micromolar to tens of micromolar in fog waters, which is much higher than the concentrations of other transition metals.[1] Due to its significant concentrations and reactivity, iron can play a crucial role in chemical transformations of dissolved organics in atmospheric aqueous phases.[4,5] Several studies have reported the degradation of soluble organics via the photolysis of iron hydroxy complexes or through the Fenton reactions in atmospheric waters.[4,6,7] The iron hydroxy complexes can undergo efficient photodissociation to form Fe(II) and ·OH under atmospherically relevant pH conditions (reactions 1 and 2), since they absorb in the near-UV region (290−400 nm).[8] The redox reaction of Fe(II) with H_2O_2 (Fenton reaction) can produce aqueous ·OH in the dark (reaction 3).

$$\mathrm{Fe(III) + H_2O \rightarrow [Fe(III)(OH)]^{2+} + H^+} \quad (1)$$

$$\mathrm{[Fe(III)(OH)]^{2+} + h\nu \rightarrow Fe(II) + \cdot OH} \quad k = 0.0012\ s^{-1} \quad (2)$$

ref[9]

$$\mathrm{Fe(II) + H_2O_2 \rightarrow Fe(III) + \cdot OH + OH^-} \quad k = 76\ M^{-1}\ s^{-1} \quad (3)$$

ref[10]

In addition to hydroxy complexes, iron can form organic complexes that are photochemically reactive and can initiate radical chain reactions. For example, a recent study has shown

Received: August 12, 2018
Revised: November 26, 2018
Accepted: November 28, 2018
Published: November 28, 2018

DOI: 10.1021/acs.est.8b04507
Environ. Sci. Technol. 2019, 53, 127−136

that the iron-carboxylato complexes formed between iron and low-molecular-weight carboxylates can have a profound impact on the iron-catalyzed photooxidation of soluble organic pollutants in atmospheric waters.[11] Carboxylates are often found in significant concentrations in atmospheric waters and tend to dominate the complexation of Fe(III) ions due to the large stability constants of such complexes.[12] Oxalate, one of the most abundant low-molecular-weight carboxylates in atmospheric waters, forms chelate complexes with Fe(III) efficiently. Zuo et al. found that Fe(III)−oxalate complexes can be the dominant species of dissolved Fe(III) in many atmospheric water samples because oxalate has a stronger affinity for Fe(III) than most of other organic ligands typically present in atmospheric droplets.[13,14] Fe(III)−oxalate complexes are typically more photoactive than "unchelated" Fe(III) ions because complexation yields a stronger absorbing chromophore, which is derived from electron transfer from oxalate ligand to iron(III).[15] The photoreactions of Fe(III)−oxalate complexes have significant implications for iron redox cycle and are potentially an important source of oxidative species in the atmosphere.

The proposed mechanisms for the photochemical/chemical generation of oxidative species from Fe(III)−oxalate complexes are shown in reactions 4−9 below.

$$[Fe(III)(C_2O_4)_3]^{3-} + h\nu \rightarrow [Fe(II)(C_2O_4)_2]^{2-} + C_2O_4^{\cdot-} \quad k = 0.04\ s^{-1} \tag{4}$$

ref[9]

$$C_2O_4^{\cdot-} \rightarrow CO_2^{\cdot-} + CO_2 \quad k = 2 \times 10^6\ s^{-1} \tag{5}$$

ref[16]

$$CO_2^{\cdot-} + O_2 \rightarrow CO_2 + O_2^{\cdot-} \quad k = 6.5 \times 10^9\ M^{-1}\ s^{-1} \tag{6}$$

ref[17]

$$O_2^{\cdot-} + H^+ \leftrightarrow HO_2\cdot \tag{7}$$

$$Fe(II) + O_2^{\cdot-}/HO_2\cdot + H^+ \rightarrow Fe(III) + H_2O_2 \quad k = 1.0 \times 10^7/1.2 \times 10^6\ M^{-1}\ s^{-1} \tag{8}$$

ref[18]

$$[Fe(II)C_2O_4] + H_2O_2 \rightarrow [Fe(III)C_2O_4]^+ + \cdot OH + OH^- \quad k = 3.1 \times 10^4 M^{-1} s^{-1} \tag{9}$$

ref[19]

Depending on the pH and the Fe(III)/oxalate ratio, oxalate forms three kinds of complex with Fe(III): $[Fe(III)(C_2O_4)]^+$, $[Fe(III)(C_2O_4)_2]^-$ and $[Fe(III)(C_2O_4)_3]^{3-}$, simultaneously in different proportions in solution.[20] $[Fe(III)(C_2O_4)_2]^-$ and $[Fe(III)(C_2O_4)_3]^{3-}$ are known to have a higher photochemical reactivity than $[Fe(III)(C_2O_4)]^+$.[21] Among Fe(III)−oxalate complexes, the photodissociation of $[Fe(C_2O_4)_3]^{3-}$ is of most intense interest and has been investigated in detail. The primary photochemical process following the excitation of $[Fe(C_2O_4)_3]^{3-}$ involves intramolecular electron transfer from oxalate to Fe(III) with formation of a primary intermediate $C_2O_4^{\cdot-}$ (reaction 4), the $C_2O_4^{\cdot-}$ radical will then dissociate to form carbon dioxide anion radical ($CO_2^{\cdot-}$) and CO_2 instantly (reaction 5).[22−24] The mechanism of photolysis of $[Fe(III)(C_2O_4)_2]^-$ and $[Fe(III)(C_2O_4)]^+$ has not been studied extensively but the reactions are assumed to produce Fe(II) and $CO_2^{\cdot-}$ eventually.[17] The subsequent reaction of $CO_2^{\cdot-}$ with O_2 leads to the formation of the intermediate superoxide ion and the hydroperoxyl radical (denoted as $O_2^{\cdot-}$/ $HO_2\cdot$), which reacts with Fe(II) to produce H_2O_2 in the acidic pH range (reactions 6−8). Finally, H_2O_2 will interact with Fe(II) (reaction 3) or with $[Fe(II)C_2O_4]$ (reaction 9) to yield $\cdot OH$.

Although the photochemistry of ferrioxalate complexes has been studied extensively, their role in the aging of atmospherically relevant species in aqueous phase is still in its infancy.[11] Thomas et al. investigated the reactive uptake and photooxidation of gas-phase glycolaldehyde on aqueous seed aerosol containing Fe(III)−oxalate complexes.[11] They found that the presence of Fe(III)−oxalate in seed aerosol inhibited the aerosol growth, which suggests that iron(III) oxalate-mediated photooxidation of glycolaldehyde leads to the formation of volatile oxidation products. Zuo et al. studied the Fe(III)-catalyzed photochemical oxidation of dissolved sulfur dioxide (SO_2) in the presence of oxalate under atmospherically relevant conditions.[25] Their results show that the presence of oxalate strongly inhibits Fe(III)-catalyzed oxidation of SO_2 both in the dark and under UV−visible light due to the formation of Fe(III)−oxalate complexes. These works alluded to the potential importance of ferrioxalate photochemistry in atmospheric waters, but more studies are needed to better understand the role that Fe(III)−oxalate complexes may play in the evolution of dissolved organics.

This study explores the photochemical oxidation of guaiacol (GUA) in the presence of Fe(III)−oxalate under acidic conditions typical for atmospheric water. Guaiacol is chosen as a model compound of phenols, which are emitted in large quantities from biomass burning.[26] This work is the first to present comprehensive mechanistic and kinetic information on the photooxidation of guaiacol by Fe(III)−oxalate complexes under conditions relevant to atmospheric water. The effects of pH, Fe(III) concentration, oxalate concentration, and dissolved oxygen on the photooxidation of guaiacol were investigated. The photodegradation mechanism and the possible oxidative products were studied by high-resolution mass spectrometry (HRMS) combined with high performance liquid chromatography (HPLC). The results obtained in this study will provide a reference for predicting the photooxidation behavior of phenolic compounds in the presence of Fe(III)−carboxylato complexes in atmospheric water.

2. EXPERIMENTAL SECTION

All photochemical experiments were conducted in a 200 mL, airtight square quartz vessel (8 cm in length, containing 100 mL solution) equipped with magnetic agitation and a bubble tube for feeding high-purity air or nitrogen. For the deaeration experiment, the solution was continuously bubbled with high-purity N_2 starting from 15 min before the reaction until the end of the photoreaction. A 500W Xe lamp was used as irradiation source to simulate sunlight outside the reactor at 4 cm distance from the reactor walls. The Xe lamp with a polychromatic spectrum of $\lambda \geq 350$ nm was selected in order to avoid the direct photolysis of GUA. The irradiance at the surface of the solutions was measured at approximately 980 W m^{-2}, which is equivalent to sunlight intensity at midlatitude summer noon, as estimated by ferrioxalate actinometry.[9,27] The solution temperature of the reaction vessel was kept at 25 ± 2 °C by means of a cooling fan during the experiment. NaCl (2.58×10^{-3} M) was added to keep the ionic strength constant throughout each experiment. The materials, reagents and

DOI: 10.1021/acs.est.8b04507
Environ. Sci. Technol. 2019, 53, 127−136

additional experimental details are provided in the Supporting Information (SI).

The concentrations of GUA and nitrobenzene were determined by HPLC.[28] The experimental error in the HPLC analytical measurements is <2% on the basis of triplicate runs. The oxidation products of GUA were analyzed and formula-assigned by an Orbitrap HRMS (mass resolution $m/\Delta m$ = 140 000) equipped with HPLC. As a control experiment, 1 mM GUA (pH 3.0) was directly infused into HRMS to investigate if autoxidation of GUA occurs in the ESI source. According to the study of Slikboer et al.,[5] catechol can be oxidized to formed hydroxylated quinone species (autoxidation product) under electrospray ionization conditions in the presence of O_2(aq). However, no autoxidation product of GUA was observed in our system. The reason may be that GUA is less susceptible to oxidation in the ESI source compared to catechol. The light absorptivity of the solution and the concentration of H_2O_2 were measured by UV−vis spectroscopy. In addition, gas chromatography/mass spectrometry (GC−MS) was applied to detect the low-molecular-weight products of reactions (e.g., methanol). All speciation calculations in this work were carried out with a chemical equilibrium calculation program, Visual MINTEQ (developed by KTH, SEED, Stockholm, Sweden). Details on the analytical procedures are given in the SI.

3. RESULTS AND DISCUSSION

3.1. Effects of Oxalate on the Dark Iron-Oxidation of GUA in Aqueous Solutions. Recently, several studies have reported that the dark reaction of Fe(III) with GUA can result in the formation of light-absorbing insoluble and soluble secondary organics in aqueous solution at pH 3 under experimental conditions representative of atmospheric water.[5,29] Figure 1 and SI Figure S1a show the UV−vis absorption spectra of the solution resulting from the dark reaction of GUA with Fe(III) at pH 3 in the presence of air. The development of a wide absorption band extending from the UV region (350 nm) to the visible region (600 nm) in the dark solution of GUA + Fe(III) is attributed to the formation of conjugated oligomer products of GUA (such as compound II in SI Figure S2).[5] The proposed reaction mechanism involves the oxidation of GUA by Fe(III) to form the corresponding phenoxy radical, which proceeds through carbon−carbon radical coupling to form guaiacol dimer and the respective diphenoquinone (SI Figure S2). Interestingly, the formation of insoluble secondary organics was not observed in the dark solution of GUA + Fe(III), maybe due to the lower concentrations of Fe(III) and GUA used in this study. However, when oxalate was mixed with the Fe(III) and GUA at pH 3, the broad absorption peak between 350 and 600 nm did not appear in the UV−vis spectrum of the solution after 2 h in the dark (Figure 1), indicating no formation of the light absorbing oligomers. Instead, the UV−vis spectrum shows an absorption tail extending into wavelength >400 nm, so is the spectrum of the Fe(III) + oxalate solution (Figure 1). This tail is attributed to the ligand-to-metal charge transfer of the Fe(III)−oxalate complexes formed in both solutions. These results revealed that the presence of oxalate inhibited the dark reaction of GUA with Fe(III), likely through reducing the concentration of available Fe(III) species due to the formation of stable Fe(III)−oxalate complexes in the dark.

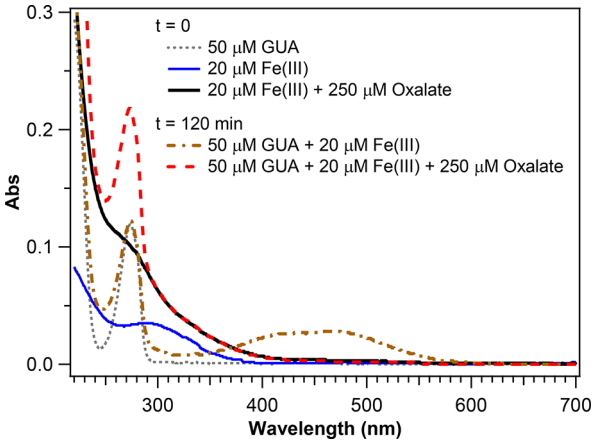

Figure 1. Comparison of UV−vis absorption spectra of solution containing 50 μM GUA, t = 0; solution containing 20 μM Fe(III), t = 0;solution containing 20 μM Fe(III) and 250 μM oxalate, t = 0; solution containing 20 μM Fe(III) and 50 μM GUA, t = 120 min;and solution containing 20 μM Fe(III), 250 μM oxalate and 50 M GUA, t = 120 min at pH 3.0 ± 0.1 in dark conditions.

Significant concentrations of oxalate have been found in rain, cloud and fog waters,[13] for which the possible sources include the dissolution of gas-phase oxalate due to its large Henry's coefficient and aqueous-phase oxidation of organic compounds. In acidic atmospheric water, oxalate ligands readily form strong chelate complexes with Fe(III) ions, thus inhibit the dark Fe(III)−oxidation of dissolved organics (such as phenols) in aqueous phase. Our results demonstrate that in the presence of carboxylic acid ligands the dark Fe(III)−oxidation pathway may be less important for the transformation of phenolic compounds in atmospheric water.

3.2. Fe(III)−Oxalate Mediated Photooxidation of GUA in Aqueous Solutions. *3.2.1. The Control Experiments.* Figure 2 shows the change of GUA concentration in aqueous solutions during the course of illumination in the presence or absence of Fe(III), and oxalate. No direct photooxidation of GUA is observed under the simulated sunlight conditions of this study (λ > 350 nm) because GUA in water does not absorb above 350 nm. In the presence of Fe(III) ions, the photooxidation of GUA occurred in the aqueous solution at pH 3. This is because $Fe(OH)^{2+}$ is the dominant Fe(III) hydroxide complexes in the aqueous solution in the pH range of 3−5 and its charge transfer band overlaps the solar UV spectrum (290−400 nm).[8] Thus, under the simulated sunlight conditions, $Fe(OH)^{2+}$ can be photolyzed to generate ·OH

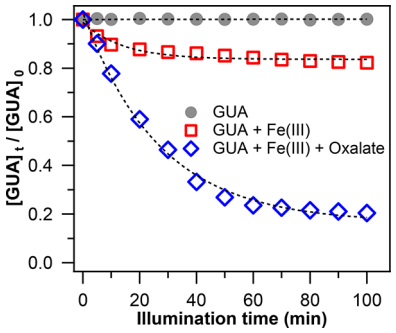

Figure 2. GUA concentration change vs time in the control experiments $[Fe(III)]_0$ = 20 μM, $[Oxalate]_0$ = 250 μM, $[GUA]_0$ = 50 μM, pH 3.0 ± 0.1, air saturated solution.

DOI: 10.1021/acs.est.8b04507
Environ. Sci. Technol. 2019, 53, 127−136

radicals (reaction 2), which react with GUA via electrophilic addition to form hydroxylated-oxidation products. Moreover, the initial photooxidation of the GUA-Fe(III) solution can be described using pseudo-first order kinetics with a rate constant of 0.004 min^{-1} (SI Figure S3). Previous studies have demonstrated that 3 is the optimum pH value for Fe(III) hydroxide complexes to produce $^{\cdot}OH$ and oxidize the organic compounds without the precipitation of Fe(III).[30,31] As shown in Figure 2, the photodegradation rate of GUA was further enhanced by adding oxalate into the aqueous solution containing GUA and Fe(III). The initial pseudo-first-order rate constant of GUA decay increased to 0.026 min^{-1}, approximately 6.5 times the rate observed in the illuminated GUA−Fe(III) solution (SI Figure S3). At the end of the irradiation (100 min), nearly 80% of the GUA in the GUA−Fe(III)−oxalate solution reacted compared to 17% in the GUA-Fe(III) solution (Figure 2). These results indicate that oxalate significantly promotes Fe-catalyzed photooxidation of GUA. The reason is that oxalate outcompetes hydroxide for complexation with Fe(III) in the acidic solution, which leads to a higher abundance of Fe(III)−oxalate complexes than Fe(III)−OH complexes in the solution and thereby alters the photoreduction pathways of Fe(III) and concomitantly the pathways of $^{\cdot}OH$ formation.[24] Indeed, previous studies have indicated that Fe(III)−oxalate complexes have a much stronger light absorbance in the tropospheric solar UV−visible region and are photochemically more reactive than inorganic Fe(III) species such as $Fe(OH)^{2+}$ in aqueous solution.[9,21] The photolysis of Fe(III)−oxalate complexes can efficiently produce $^{\cdot}OH$ in the presence of dissolved oxygen via a series of reactions (reactions 3−9), and the production rate is much higher than that of the Fe(III)−OH complexes.[31,32] The steady-state concentrations of $^{\cdot}OH$ generated by photolysis of Fe(III)−oxalate complexes and Fe(III)−OH complexes were measured employing nitrobenzene (NB) as a $^{\cdot}OH$ trap.[33] The photodegradation of NB can be described using pseudo-first-order kinetics in terms of [NB] and the concentration of $^{\cdot}OH$ was estimated using the following equations:

$$\ln \frac{[NB]_0}{[NB]_t} = kt = k_{NB,OH}[\cdot OH]t \quad (10)$$

$$[\cdot OH] = \frac{k}{k_{NB,OH}} \quad (11)$$

Where $[NB]_0$ is initial NB concentration, $[NB]_t$ is NB concentration at irradiation time t, and k and $k_{NB,OH}$ (= 3×10^9 M^{-1} s^{-1})[34] are the pseudo-first-order and second-order rate constants of NB reaction with $^{\cdot}OH$, respectively.

Figure S4 shows the photodegradation of NB in the presence of Fe(III)−oxalate complexes and in the presence of Fe(III)−OH complexes. The degradation rate constant of NB in Fe(III)−oxalate system was found to be 0.045 min^{-1}, based on eq 11, $[^{\cdot}OH]$ was calculated to be 2.5×10^{-13} M. Similarly, $[^{\cdot}OH]$ was calculated to be 1.17×10^{-13} M in the irradiated Fe(III)−OH system. Hence, a higher efficiency of photooxidation of GUA was achieved in the aqueous solution containing Fe(III)−oxalate complexes compared to that containing the Fe(III)−OH complexes.

3.2.2. Effects of Oxalate Concentration on the Fe(III)−oxalate Mediated Photooxidation of GUA in Aqueous Solutions. The effect of oxalate concentration on the photooxidation of GUA was investigated from 20 to 250 μM at a constant Fe(III) concentration of 20 μM and pH 3.0 under the simulated sunlight conditions. The photooxidation of GUA at different oxalate concentration is presented in Figure 3a as a function of irradiation time. The results indicate

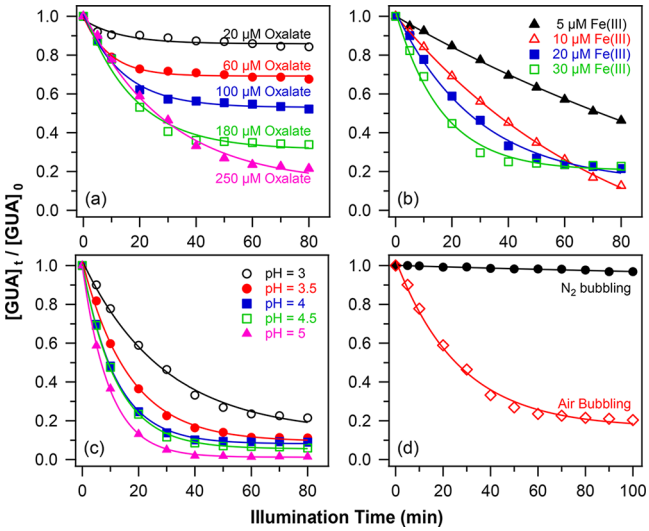

Figure 3. (a). Effect of oxalate concentration on the Fe(III)−oxalate mediated photooxidation of GUA. $[Fe(III)]_0$ = 20 μM, $[GUA]_0$ = 50 μM, pH 3.0 ± 0.1, air saturated solution; (b). Effect of Fe(III) concentration on the Fe(III)−oxalate mediated photooxidation of GUA. $[Oxalate]_0$ = 250 μM, $[GUA]_0$ = 50 μM, pH 3.0 ± 0.1, air saturated solution; (c). Effect of solution pH on the Fe(III)−oxalate mediated photooxidation of GUA. $[Fe(III)]_0$ = 20 μM, $[Oxalate]_0$ = 250 μM, $[GUA]_0$ = 50 μM, air saturated solution; (d). Effect of the presence of oxygen on the Fe(III)−oxalate mediated photooxidation of GUA. $[Fe(III)]_0$ = 20 μM, $[Oxalate]_0$ = 250 μM, $[GUA]_0$ = 50 μM, pH 3.0 ± 0.1, air bubbling, nitrogen bubbling.

that an increasing concentration of oxalate, or molar ratio of oxalate to Fe(III), leads to a significant increase of the photooxidation efficiency of GUA. For example, the most effective degradation was observed at an oxalate concentration of 250 μM with a loss of ≈80% of GUA after 80 min of illumination. The increase in degradation efficiency of GUA was due to the formation of Fe(III)−oxalate complexes that were photolyzed to yield oxalate radicals ($C_2O_4^{\cdot -}$) triggering $^{\cdot}OH$ formation in the presence of dissolved oxygen (reactions 3, 5−9). Thus, increasing the concentration of oxalate enhances the yield of $^{\cdot}OH$ and concomitantly the degradation efficiency of GUA.

The initial photooxidation rate of GUA depended on the oxalate/Fe(III) molar ratio as well, although not monotonically. As shown in SI Figure S5, the GUA photooxidation followed pseudo-first order kinetics during the first 30 min of illumination and the rate increased with the oxalate/Fe(III) molar ratio between 1 and 9 but decreased from 9 to 12.5. This can be explained by the dependence of the speciation of Fe(III) complexes on oxalate concentration. As shown in SI Figure S6, at lower oxalate/Fe(III) molar ratio (e.g., 1:1), Fe(III) is mainly present as $[Fe(C_2O_4)]^+$ and $[Fe(OH)]^{2+}$, but the major Fe(III) complexes shift to $[Fe(C_2O_4)_2]^-$ and $[Fe(C_2O_4)_3]^{3-}$ at a high oxalate/Fe(III) molar ratio of 9. Since $[Fe(C_2O_4)_2]^-$ and $[Fe(C_2O_4)_3]^{3-}$ are much more photoactive than $[Fe(C_2O_4)]^+$ and $[Fe(OH)]^{2+}$, the formation rate of $^{\cdot}OH$, and therefore the photooxidation rate of GUA, becomes faster at higher oxalate concentration. But a lower

DOI: 10.1021/acs.est.8b04507
Environ. Sci. Technol. 2019, 53, 127−136

initial degradation rate of GUA at oxalate concentration of 250 μM compared to 180 μM (SI Figure S5) suggests that excess oxalate inhibits the degradation of GUA initially. The reason may be that oxalate can also act as a scavenger of $^{\cdot}OH$ produced in the Fenton reaction (reaction 3 or 9) and hence competes with GUA for $^{\cdot}OH$ and significantly inhibits the degradation of GUA at high oxalate concentration.[9] However, such inhibition effect declines with the consumption of oxalate.

3.2.3. Effects of Fe(III) Concentration on the Fe(III)–oxalate Mediated Photooxidation of GUA. To investigate the effect of Fe(III) concentration on the photooxidation of GUA, solutions at pH 3.0 containing 5–30 μM Fe(III), 250 μM oxalate, and 50 μM GUA were irradiated with simulated sunlight. Figure 3b shows the time-variation of the concentration of GUA at different Fe(III) concentration. The photooxidation rate of GUA increased with Fe(III) concentration from 5 to 30 μM during the first 30 min of reaction and the pseudo-first order photooxidation rate constant of GUA increased from 0.008 to 0.041 min^{-1} (SI Figure S7). Since a single Fe(III) ion can complex a number of oxalate ligand in the solution and oxalate was used in excess to Fe(III) in our experiments, increasing Fe(III) concentration enhances the concentration of Fe(III)–oxalate complexes, which leads to a higher H_2O_2 and Fe(II) concentrations due to ferrioxalate photolysis and concomitantly a higher $^{\cdot}OH$ concentration resulting from the Fenton reaction. However, when the reaction lasted for more than 1 h, the most effective degradation was achieved at a Fe(III) concentration of 10 μM rather than 30 μM (Figure 3b). The difference between the red curve (10 uM) and the green curve (30uM) at 80 min was statistically significant, which was unlikely the outcome of experimental errors (<2%). The reason may be that the competition reactions occurred between ferrioxalate and dissolved O_2 for $CO_2^{\cdot-}$ when Fe(III) concentration was relative high. At low concentration of ferrioxalate, $CO_2^{\cdot-}$ mainly reacted with dissolved O_2, contributing to the formation of H_2O_2 and $^{\cdot}OH$, whereas at high concentration of ferrioxalate, a majority of $CO_2^{\cdot-}$ interacted with ferrioxalate, resulting in the formation of Fe(II) and CO_2 (reaction 12).[35] Thus, with the increase in Fe(III) concentration, more $CO_2^{\cdot-}$ would reduce Fe(III) to Fe(II) rather than react with O_2 to form H_2O_2, which leads to a decrease in $^{\cdot}OH$ yield and degradation efficiency of GUA.

$$[Fe(III)(C_2O_4)_3]^{3-} + CO_2^{\cdot-} \rightarrow [Fe(II)(C_2O_4)_2]^{2-} + CO_2 + C_2O_4^{2-} \quad (12)$$

3.2.4. Effects of Solution pH on the Fe(III)–oxalate Mediated Photooxidation of GUA. The solution pH has a profound effect on the speciation and reactivity of iron-catalyzed oxidative processes. The pH value in acidic atmospheric water typically ranges from 3 to 5.[13] Therefore, experiments were carried out on the air-bubbled solution containing 20 μM Fe(III), 250 μM oxalate, and 50 μM GUA with the pH adjusted from 3 to 5 to test the effects of pH on the photooxidation of GUA under simulated sunlight irradiation. As shown in Figure 3c, the photooxidation rate of GUA increased with increasing pH between 3.0 and 5.0. Besides, the photooxidation of GUA at different pH values followed pseudo-first order reaction and the rate constants increased from 0.026 to 0.099 min^{-1} with the increase of pH value from 3 to 5 (SI Figure S8). The pH-dependence of GUA degradation in the photo/ferrioxalate system can be explained by the dependence of Fe(II) speciation on pH value, which affects the rate of the Fenton reaction. Free Fe(II) ions, the dominant Fe(II) species at low pH, reacts with H_2O_2 at a rate constant of 76 M^{-1} s^{-1} (Reaction c in Table 1). With the increase of solution pH, the concentration of $[Fe(II)(C_2O_4)]$ increases and $[Fe(II)(C_2O_4)]$ is oxidized by H_2O_2 at a rate constant of 3.1×10^4 M^{-1} s^{-1} (Reaction d in Table 1). Thus, the Fenton reaction is much faster at higher pH value. Furthermore, pH affects the reactions of active intermediates $O_2^{\cdot-}/HO_2^{\cdot}$ with Fe(II), which represent a main source of H_2O_2 in Fe(III)–oxalate system. Thus, pH value has an important effect on the formation of H_2O_2. In addition, there are several competitive reactions of $O_2^{\cdot-}/HO_2^{\cdot}$ with iron species (Reactions e–h listed in Table 1). Among them, the reactions between free Fe(III) ions and $O_2^{\cdot-}/HO_2^{\cdot}$ could be ignored in spite of their high rate constants, since a 10-fold (molar) excess of oxalate/Fe(III) used in this study ensured that almost all of Fe(III) presented as Fe(III)–oxalate complexes rather than free Fe(III) ions. Besides, the reactions between Fe(III)–oxalate complexes and $O_2^{\cdot-}/HO_2^{\cdot}$ also became negligible as the photoreduction of Fe(III)–oxalate complexes took place at much faster rates than the reduction of the Fe(III)–oxalate complexes by $O_2^{\cdot-}/HO_2^{\cdot}$.[19] Thus, the formation of H_2O_2 was mainly governed by the reactions of $O_2^{\cdot-}/HO_2^{\cdot}$ with Fe(II). In the lower pH range, $HO_2^{\cdot}$ was the dominant species, while with the increase of pH value, $O_2^{\cdot-}$ became more important.[13] The production of H_2O_2 through the Fe(II) + $O_2^{\cdot-}$ reaction is nearly an order of magnitude faster than that through the Fe(II) + $HO_2^{\cdot}$ reaction (Reactions a and b in Table 1). Therefore, the increase in pH value led to faster $^{\cdot}OH$ generation and concomitantly greater GUA degradation.

Table 1. Reactions and Reaction Rate Constants for Fe(II)/Fe(III) with $HO_2^{\cdot}/O_2^{\cdot-}$ and H_2O_2 in Aqueous Phase

no.	reaction	k (M^{-1} s^{-1})	ref
a	$Fe(II) + HO_2^{\cdot} + H^+ \rightarrow Fe(III) + H_2O_2$	1.2×10^6	18
b	$Fe(II) + O_2^{\cdot-} + H^+ \rightarrow Fe(III) + H_2O_2$	1.0×10^7	18
c	$Fe(II) + H_2O_2 \rightarrow Fe(III) + OH^{\cdot} + OH^-$	76	10
d	$[Fe(II)C_2O_4] + H_2O_2 \rightarrow [Fe(III)C_2O_4]^+ + OH^{\cdot} + OH^-$	3.1×10^4	19
e	$Fe(III) + HO_2^{\cdot} \rightarrow Fe(II) + O_2 + H^+$	$<1 \times 10^4$	18
f	$Fe(III) + O_2^{\cdot-} \rightarrow Fe(II) + O_2$	1.5×10^8	18
g	$[Fe(III)(C_2O_4)_n]^{3-2n} + HO_2^{\cdot} \rightarrow [Fe(II)(C_2O_4)_n]^{2-2n} + O_2 + H^+$	$<1.2 \times 10^5$	19
h	$[Fe(III)(C_2O_4)_n]^{3-2n} + O_2^{\cdot-} \rightarrow [Fe(II)(C_2O_4)_n]^{2-2n} + O_2$	$<1 \times 10^6$	19
i	$Fe(III) + H_2O_2 \rightarrow Fe(II) + O_2 + H^+$	very slow	10

3.2.5. Effects of the Presence of Oxygen on the Fe(III)–oxalate Mediated Photooxidation of GUA. In order to determine the effect of dissolved oxygen on the Fe-catalyzed photooxidation of GUA, photochemical experiments were conducted on the air- or nitrogen-saturated solutions containing 20 μM Fe(III), 250 μM oxalate, and 50 μM GUA at pH 3.0. As shown in Figure 3d, only a slight decrease of GUA concentration was observed in the solution saturated with nitrogen after 100 min of simulated sunlight irradiation, which suggests the Fenton reaction pathways were inactive. In contrast, the concentration of GUA decreased significantly in the presence of air, which means that the oxidation of GUA in the irradiated ferrioxalate system needs the participation of oxygen. In addition, as shown in SI Figure S9, the concentration of H_2O_2 in the air-saturated solution increased

DOI: 10.1021/acs.est.8b04507
Environ. Sci. Technol. 2019, 53, 127–136

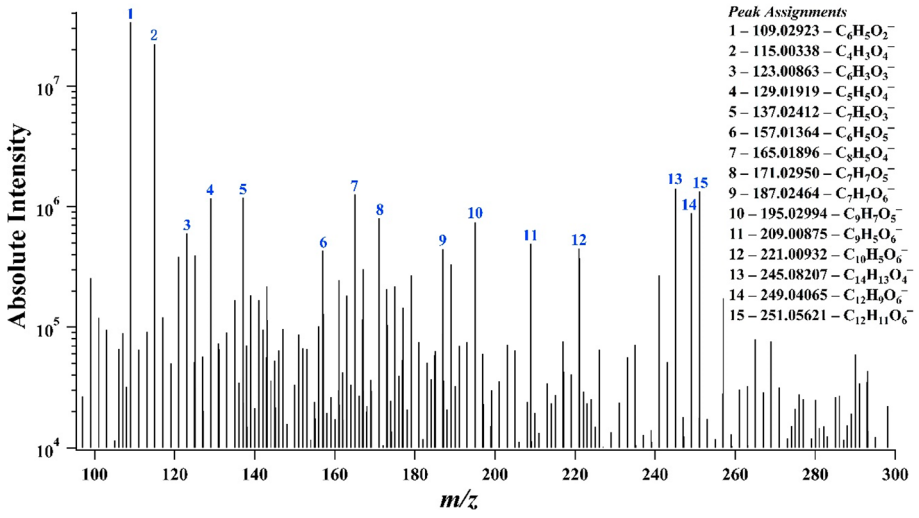

Figure 4. Orbitrap mass spectrum the oxidative products of GUA from the photo/ferrioxalate system: $[Fe(III)]_0$ = 20 μM, $[oxalate]_0$ = 250 μM, $[GUA]_0$ = 50 μM, pH 3.0 ± 0.1, air bubbling. The mass spectrum was acquired in negative electrospray ionization modes. The proposed chemical structures for the compounds identified in Figure 4 are presented in SI Table S1.

continuously during the first 50 min then dropped off from 50 to 100 min whereas H_2O_2 was below the detection limit (<0.1 μM) in the N_2-saturated solution during the entire experiment. These results stress the necessity of oxygen for the generation of H_2O_2 and ·OH by photodissociation of Fe(III)−oxalate complexes.

The photolysis of Fe(III)−oxalate complex resulted in the reduction of Fe(III) to Fe(II) and the formation of $CO_2^{\cdot-}$, which is a powerful reducing agent and could reduce another Fe(III)−oxalate ion or the dissolved O_2 depending on the relative concentrations of ferrioxalate to oxygen in the solution.[35] In air-saturated solution, the concentration of dissolved O_2 was about 250 μM, much higher than the 20 μM Fe(III) ion used in this study, thus $CO_2^{\cdot-}$ would preferentially reduce O_2 to $O_2^{\cdot-}$ rather than react with ferrioxalate to produce Fe(II).[25] The $O_2^{\cdot-}$ and its conjugate acid (i.e., HO_2•) mainly reacted with Fe(II) to form H_2O_2 (reaction 8), which subsequently interacted with Fe(II) (reaction 3) or [Fe(II)-C_2O_4] (reaction 9) to produce ·OH. In the absence of oxygen, $CO_2^{\cdot-}$ can also react with GUA,[36] which explains the slight decline of GUA in the N_2-bubbling experiment (Figure 3d).

3.3. The Photooxidation Pathways of GUA in the Presence of Fe(III)−oxalate Complexes. Based on the molecular information obtained through the Orbitrap HRMS analysis, we elucidate the photooxidation mechanisms of GUA in Fe(III)−oxalate mediated systems. In the irradiated Fe(III)−oxalate system, attack by ·OH was the predominant pathway for GUA degradation, whereas the other reactive oxygen species (e.g., $O_2^{\cdot-}$/HO_2·, H_2O_2) generated played an insignificant role in GUA degradation due to their lower reactivity toward phenols.[37] Previous studies have demonstrated that ·OH plays a vital role in the transformation of dissolved organic pollutants in atmospheric water.[2,38] In general, ·OH reacts with aromatic compounds via three channels: electron transfer, hydrogen atom abstraction and electrophilic addition. These reactions result in the substantial formation of low-volatility materials from GUA. For phenolic compounds such as GUA, electrophilic addition of ·OH to the aromatic ring usually prevails over the other two channels.[36,39] H-abstraction from phenolic hydroxyl groups and methoxy groups is typically slow and H-abstraction from the aromatic ring is always a very minor reaction pathway. Electron transfer is a less common pathway because it requires very electron-rich matrices.[39−41]

Figure 4 shows the Orbitrap mass spectra of the oxidative products formed in the GUA-Fe-oxalate solution after irradiation for 100 min. Note that a majority of the smaller and more oxidized ring-opening products are not included in Figure 4 as the mass spectra were acquired only for the range of m/z 90−500. The Van Krevelen diagram (SI Figure S10) reveals the presence of a large number of molecules with double bond equivalent (DBE) > 5, suggesting that they contain at least one aromatic ring. SI Table S1 lists 40 key molecules identified as the products of GUA photooxidation, including hydroxylated species, aldehydes, acids, esters, oligomers, epoxide, hydroperoxide, and quinone. For example, the ions at m/z = 139.03976 ($C_7H_7O_3^-$) and m/z = 261.07693 ($C_{14}H_{13}O_5^-$) suggested the presence of hydroxylated GUA and hydroxylated GUA dimer, respectively. Poly hydroxylated products were also identified, as the ions at m/z = 171.02946 ($C_7H_7O_5^-$) and m/z = 187.02462 ($C_7H_7O_6^-$) were assigned to the low-volatility products, that is, trihydroxy and tetrahydroxy guaiacol, respectively. These results indicate that hydroxylation was a significant reaction pathway that led to the oxidation of GUA. Oligomerization was another reaction channel that contributed to the transformation of GUA (SI Table S1). The high abundance of ions at m/z = 245.08215 ($C_{14}H_{13}O_4^-$) and m/z = 243.06636 ($C_{14}H_{11}O_4^-$) in the HRMS indicates the presence of guaiacol dimer and its derivative (Figure 5, A_{16}, A_{17}, A_{18}). However, ions representing trimer and higher oligomer were not detected at significant signal-to-noise ratios in the HRMS, implying that the products were highly oxygenated in the irradiated Fe(III)−oxalate system. According to the study of Yu et al.,[42] the GUA oligomers are intermediate products mainly formed in the initial stage of OH- mediated reactions. As the reaction proceeds, longer aging can lead to the fragmentation of oligomers, forming more oxygenated and smaller products.[42]

The HRMS results revealed the ubiquitous formation of acid, esters, epoxide, hydroperoxide, quinone from GUA as well. For example, the noticeable peaks at m/z = 179.03482 ($C_9H_7O_4^-$) and m/z = 195.02994 ($C_9H_7O_5^-$) in the HRMS of

DOI: 10.1021/acs.est.8b04507
Environ. Sci. Technol. 2019, 53, 127−136

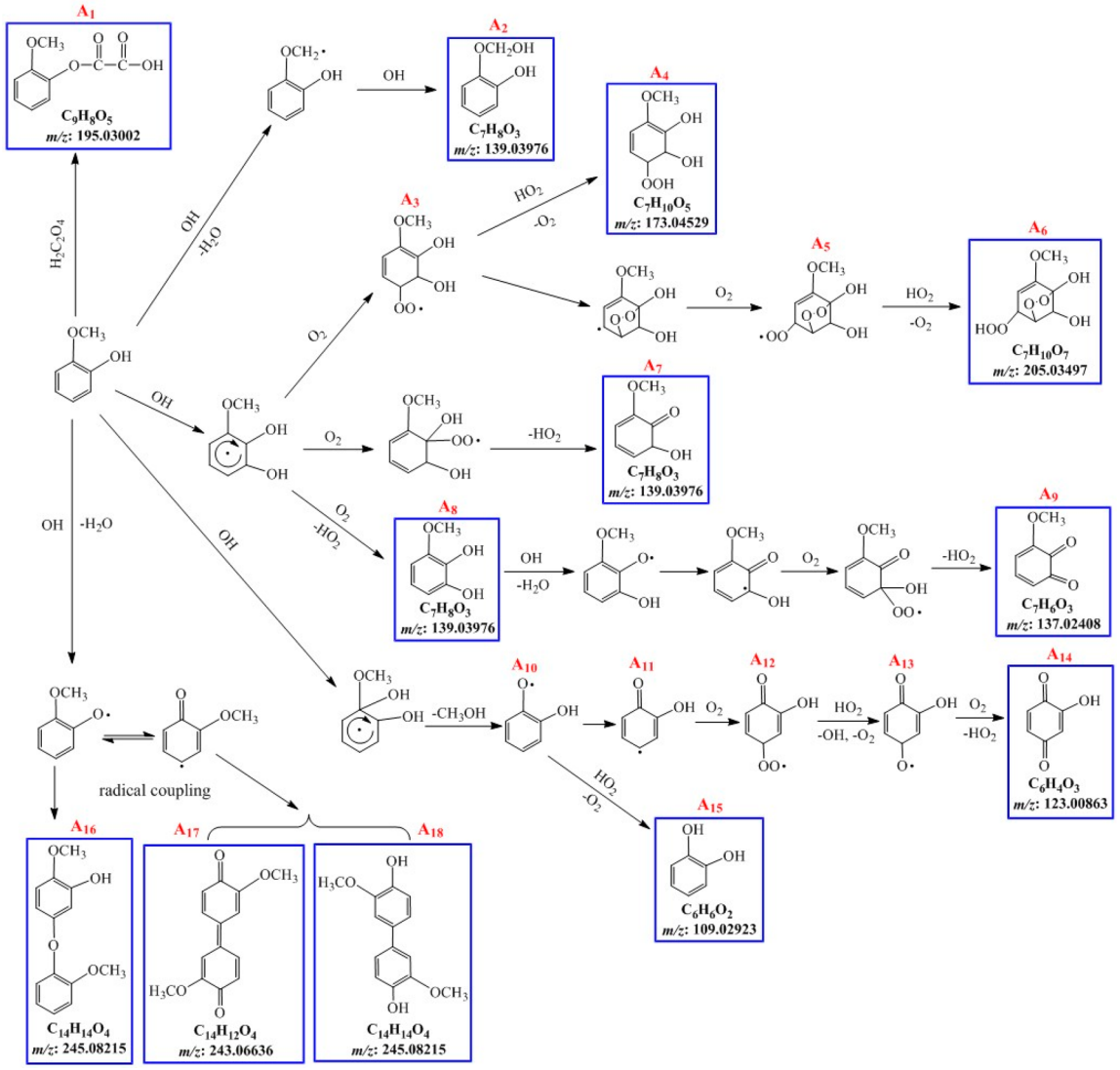

Figure 5. Proposed mechanisms for the formation of hydroxylated species, dimers esters, quinones, ketones, hydroperoxide, and demethoxylated products from aqueous reactions of GUA with OH radical generated by the photolysis of Fe(III)−oxalate complexes. All the species produced via the reactions of GUA with OH may undergo further ring-opening processes to form ketones, aldehyde, epoxide, and carboxylic acids. Compounds highlighted in blue boxes were detected by Orbitrap−MS.

the products suggested the formation of two kinds of guaiacol esters, 2-methoxy phenyl glyoxylate and 2-methoxy phenyl oxalate. The peak at m/z = 205.03497 ($C_7H_9O_7^-$) implied the presence of highly oxidized species bicyclic hydroperoxide (Figure 5, A_6). The pronounced signal at m/z = 123.00863 ($C_6H_3O_3^-$) was assigned to hydroxybenzoquinone, which was likely a demethoxylated aromatic product of GUA oxidation. Interestingly, demethoxylation of GUA by ·OH also led to the formation of dihydroxybenzene (catechol), a marker for biomass burning, corresponding to the strong signal at m/z = 109.02923 ($C_6H_5O_2^-$). The peak at m/z = 171.02946 ($C_7H_7O_5^-$) represented a ring-cleavage epoxy product of GUA oxidation (Figure 6, B_5). Besides, a large number of low-molecular-weight products (number of C atoms <6), such as $C_4H_3O_4^-$ at m/z = 115.00338 and $C_5H_5O_4^-$ at m/z = 129.01919, were identified. These small organic acids were highly oxygenated open-ring products of GUA.

Based on the above results, we proposed in Figure 5 the main pathways of GUA oxidation through the reactions with ·OH. Briefly, the reactions with organic acids can lead to the esterification of GUA.[43] For example, the reaction between GUA and oxalic acid produces a phenolic ester−methoxyphenyl oxalate (A_1). H-abstraction from the methoxy group of GUA by ·OH, followed by ·OH addition to OCH_2 radical group, results in the formation of a hemiacetal (A_2), which is a minor route for GUA oxidation by ·OH.[44] The electrophilic *ortho*-addition of ·OH to the aromatic ring of GUA, followed by O_2 addition, leads to the formation of the primary peroxy radical (A_3), which can react with HO_2 to form guaiacol hydroperoxide (A_4). The primary peroxy radical (A_3) can also isomerize to form bicyclic peroxy radical (A_5), which will proceed through H-abstraction from HO_2 to form bicyclic hydroperoxide (A_6). The *ortho*-addition of ·OH to the ring, followed by O_2 addition and HO_2 elimination, results in the formation of 2-hydroxy-6-methoxy-3,5-cyclohexadienone (A_7) and monohydroxy guaiacol (A_8). A_8 can be further oxidized to form 2-methoxy-o-quinone (A_9) through H-abstraction from hydroxyl groups by ·OH, O_2 addition, then HO_2 elimination. In addition, H-abstraction from phenolic hydroxyl groups of GUA by ·OH leads to the formation of phenoxy radical, which

DOI: 10.1021/acs.est.8b04507
Environ. Sci. Technol. 2019, 53, 127−136

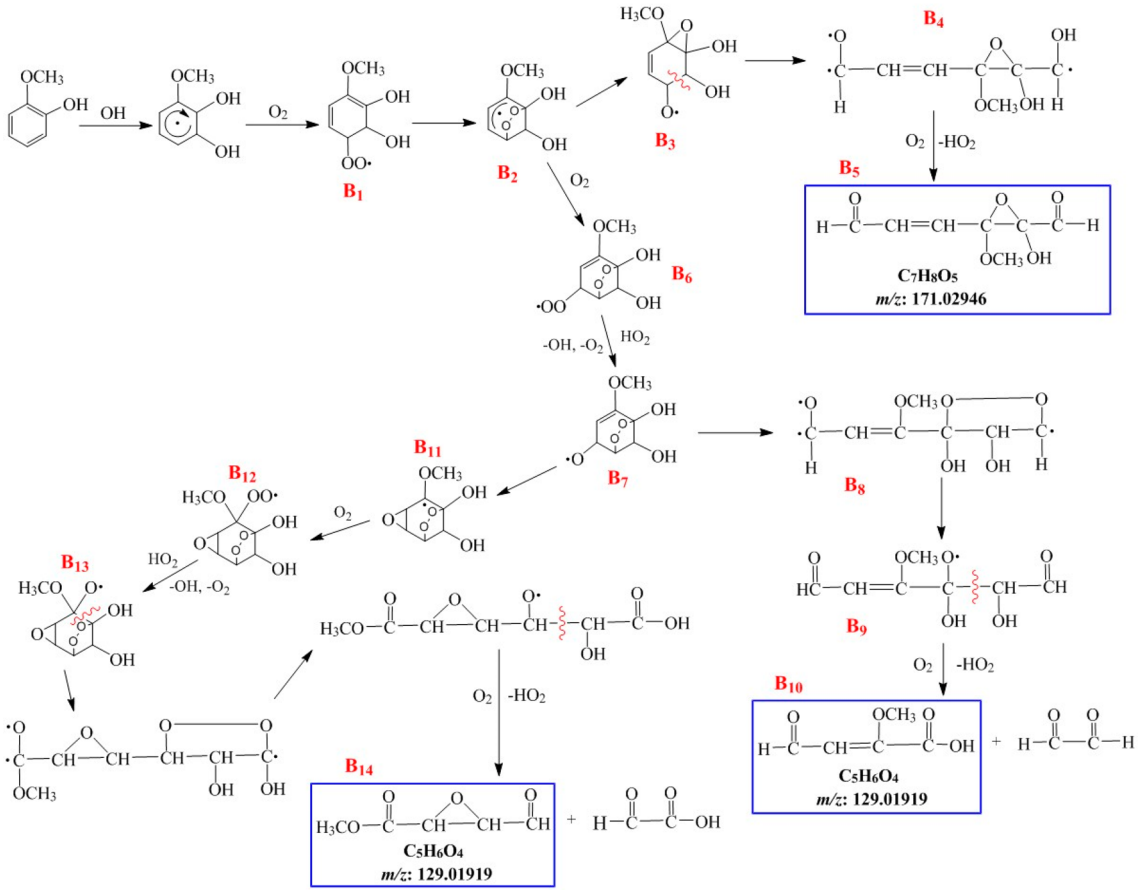

Figure 6. Proposed ring-opening mechanisms for the reaction of GUA with OH radical generated by the photolysis of Fe(III)−oxalate complexes. Compounds highlighted in blue boxes were detected by Orbitrap−MS.

is known to undergo radical recombination via C−C or C−O coupling in aqueous phase to form dimers (A_{16}, A_{17} and A_{18}).[45] Demethoxylation occurs through electrophilic *ipso*-addition of ·OH to ring positions occupied by methoxyl groups, followed by elimination of a methanol molecule to yield semiquinone radicals (A_{10}).[46] A_{10} can directly interact with HO_2 to form dihydroxybenzene (A_{15})[44,47] or isomerize to form alkyl radical (A_{11}). A_{11} reacts rapidly with O_2 to yield peroxy radical (A_{12}), which is then reduced to alkoxy radical (A_{13}) by HO_2. A_{13} will further undergo H-abstraction by O_2 to yield 2-hydroxy-p-benzoquinone (A_{14}). This demethoxy route eventually leads to carbon loss from methoxyphenol system and converts methoxy groups to hydroxyl or carbonyl groups. To further confirmed the occurrence of the methoxy loss route, we employed GC−MS to identify methanol in the photooxidation products of GUA and unambiguously detected methanol in the products (SI Figure S11). According to the study of Aihara et al.,[44] *ipso*-addition of ·OH is a more important route compared to *ortho*- and *para*-addition of ·OH to the ring of methoxyphenol in aqueous phase, so *ipso*-addition of ·OH may be a major route that leads to the oxidation of GUA in current systems.

Furthermore, the reactants and products from all these reaction pathways can further undergo ring opening and fragmentation processes, resulting in the substantial formation of aldehyde, ketone, epoxide and carboxylic acid. Since almost all low-volatility small molecules (C number <6) in the oxidative products of aromatics originate from the open-ring processes, the ring-opening reactions initiated by ·OH play a significant role in producing aromatic SOA in both gas phase and liquid phase. The OH-mediated ring-opening oxidation mechanisms for gas-phase aromatic organics have been investigated extensively, but very little is known for the liquid-phase reactions of aromatics. Figure 6 shows the ring-opening oxidative mechanisms of GUA mediated by ·OH in water. The addition of ·OH and O_2 to the aromatic ring of GUA leads to the formation of primary peroxy radical (B_1), which would preferably cyclize to the bicyclic allyl radical (B_2) since the allylically stabilized five-membered bicyclic radicals are the lowest energy radicals formed.[48,49] The bicyclic intermediate B_2 is the source for the reaction pathways that lead to the formation of ring-opening products.[50] B_2 will go on to react via two channels. One channel is to break the −O−O− bond of B_2 to form epoxy alkoxy radicals (B_3). The breakage of the aromatic ring on B_3 produces epoxide-containing radical product (B_4), which undergoes H-abstraction by O_2 to yield the unsaturated epoxy-1,6-dicarbonyl (B_5) eventually.[51] In the other channel, B_2 combines with O_2 to produce bicyclic peroxy radical (B_6), which is reduced to a bicyclic alkoxy radical (B_7) by HO_2. B_7 subsequently undergoes two contrary processes: ring-breakage or ring-closure. The β-scission of B_7 gives the ring-open radical product (B_8), which breaks the −O-O- bond to form a radical (B_9). B_9 then decomposes via the C−C scission to ultimately form glyoxal and highly oxygenated unsaturated carboxylic acid (B_{10}). It is important to note that the scission occurs preferably at the C−C bond between the carbon with the oxygen atom attached to it and the saturated carbon center.[49] The ring-closure of B_7 produces bicyclic epoxyl radical (B_{11}), which then

DOI: 10.1021/acs.est.8b04507
Environ. Sci. Technol. 2019, 53, 127−136

recombines with O_2 to form bicyclic epoxyl peroxy radical (B_{12}). B_{12} would react with HO_2 to form bicyclic epoxyl alkoxy radical (B_{13}), which is subject to C−C bond breakages and to H-abstraction by O_2 to eventually yield glyoxylic acid and highly oxidized epoxy-1,4-dicarbonyl (B_{14}).[52] These results reveal that OH-mediated ring-opening reactions of GUA in liquid phase may be a significant source of small-molecular products such as glyoxal, glyoxylic acid as well as highly oxidized species in the atmosphere. Note that the ring-opening mechanisms mediated by ·OH are also applicable to other oxidized products containing aromatic ring in current reaction system.

4. ENVIRONMENTAL SIGNIFICANCE

We studied the importance of Fe and oxalate in the aqueous aging of GUA. For the dark reaction, the presence of oxalate inhibits the Fe(III)−oxidation of GUA. For the photoreaction, the presence of oxalate can strongly promote the Fe-catalyzed oxidation of GUA via the formation of photoactive Fe(III)−oxalate complexes which can undergo efficient photodissociation to produce ·OH under simulated sunlight. The photodegradation rate and efficiency of GUA increase with the increase of pH value from 3 to 5. By using high resolution mass spectrometry, a large number of products with different degrees of oxidation (including dimers and their related derivatives, ring-opening products, functionalized products) were identified. The reaction mechanism is proposed in detail based on the molecular analysis by HRMS.

It is expected that the formation of oxidants in atmospheric water by photolysis of Fe(III)−oxalate complexes is continuous since oxalate are continuously replenished by gas-to-liquid partitioning and in-cloud oxidation of other organic matters. In addition to oxalate, other organic acids in atmospheric water such as pyruvate and glyoxalate can form complexes with Fe(III) and these Fe(III)−organic complexes have been reported to generate reactive oxidative species such as ·OH and H_2O_2.[13,53] Although we only focused on the role that the Fe(III)−oxalate complexes play in the chemical evolution of GUA, other Fe(III)−organic complexes may also play a significant role in the degradation of GUA and other soluble organics in atmospheric aqueous phase. Therefore, our work implies that the Fe(III)−organic complexes are potentially a powerful source of oxidants in atmospheric condensed phases and play a significant role in the transformation of the dissolved organic compounds in the atmosphere.

■ ASSOCIATED CONTENT

Supporting Information

The Supporting Information is available free of charge on the ACS Publications website at DOI: 10.1021/acs.est.8b04507.

Materials and reagents, additional experimental details, analytical procedures, Figure S1−S11 and Table S1 (PDF)

■ AUTHOR INFORMATION

Corresponding Authors

*(X.L) E-mail: luxiaohui@fudan.edu.cn.

*(X.Y.) E-mail: yangxin@fudan.edu.cn.

ORCID

Qi Zhang: 0000-0002-5203-8778

Li Li: 0000-0001-5575-0894

Xin Yang: 0000-0002-9173-1188

Notes

The authors declare no competing financial interest.

■ ACKNOWLEDGMENTS

This work was supported by the National Natural Science Foundation of China (Nos. 91544224, 21507010, 41775150, 41827804). Q.Z. also acknowledges the funding from the National Science Foundation grant number AGS-1649212.

■ REFERENCES

(1) Deguillaume, L.; Leriche, M.; Desboeufs, K.; Mailhot, G.; George, C.; Chaumerliac, N. Transition metals in atmospheric liquid phases: Sources, reactivity, and sensitive parameters. *Chem. Rev.* **2005**, *105* (9), 3388−3431.

(2) Herrmann, H.; Schaefer, T.; Tilgner, A.; Styler, S. A.; Weller, C.; Teich, M.; Otto, T. Tropospheric aqueous-phase chemistry: kinetics, mechanisms, and its coupling to a changing gas phase. *Chem. Rev.* **2015**, *115* (10), 4259−4334.

(3) Al-Abadleh, H. Review on the Bulk and Surface Chemistry of Iron in Atmospherically-Relevant Systems Containing Humic like Substances. *RSC Adv.* **2015**, *5*, 45785−45811.

(4) Deng, Y.; Zhang, K.; Chen, H.; Wu, T.; Krzyaniak, M.; Wellons, A.; Bolla, D.; Douglas, K.; Zuo, Y. Iron-catalyzed photochemical transformation of benzoic acid in atmospheric liquids: Product identification and reaction mechanisms. *Atmos. Environ.* **2006**, *40* (20), 3665−3676.

(5) Slikboer, S.; Grandy, L.; Blair, S. L.; Nizkorodov, S. A.; Smith, R. W.; Al-Abadleh, H. A. Formation of light absorbing soluble secondary organics and insoluble polymeric particles from the dark reaction of catechol and guaiacol with Fe (III). *Environ. Sci. Technol.* **2015**, *49* (13), 7793−7801.

(6) Moonshine, M.; Rudich, Y.; Katsman, S.; Graber, E. Atmospheric HULIS enhance pollutant degradation by promoting the dark Fenton reaction. *Geophys. Res. Lett.* **2008**, *35* (20), L20807.

(7) Nguyen, T.; Coggon, M.; Flagan, R.; Seinfeld, J. Reactive uptake and photo-fenton oxidation of glycolaldehyde in aerosol liquid water. *Environ. Sci. Technol.* **2013**, *47* (9), 4307−4316.

(8) Feng, W.; Nansheng, D. Photochemistry of hydrolytic iron (III) species and photoinduced degradation of organic compounds. A minireview. *Chemosphere* **2000**, *41* (8), 1137−1147.

(9) Balmer, M. E.; Sulzberger, B. Atrazine degradation in irradiated iron/oxalate systems: effects of pH and oxalate. *Environ. Sci. Technol.* **1999**, *33* (14), 2418−2424.

(10) Walling, C. Fenton's reagent revisited. *Acc. Chem. Res.* **1975**, *8* (4), 125−131.

(11) Thomas, D. A.; Coggon, M. M.; Lignell, H.; Schilling, K. A.; Zhang, X.; Schwantes, R. H.; Flagan, R. C.; Seinfeld, J. H.; Beauchamp, J. L. Real-Time Studies of Iron Oxalate-Mediated Oxidation of Glycolaldehyde as a Model for Photochemical Aging of Aqueous Tropospheric Aerosols. *Environ. Sci. Technol.* **2016**, *50* (22), 12241−12249.

(12) Weller, C.; Horn, S.; Herrmann, H. Photolysis of Fe (III) carboxylato complexes: Fe (II) quantum yields and reaction mechanisms. *J. Photochem. Photobiol., A* **2013**, *268*, 24−36.

(13) Zuo, Y.; Hoigne, J. Formation of hydrogen peroxide and depletion of oxalic acid in atmospheric water by photolysis of iron (III)-oxalato complexes. *Environ. Sci. Technol.* **1992**, *26* (5), 1014−1022.

(14) Zuo, Y. Kinetics of photochemical/chemical cycling of iron coupled with organic substances in cloud and fog droplets. *Geochim. Cosmochim. Acta* **1995**, *59* (15), 3123−3130.

(15) Mangiante, D. M.; Schaller, R. D.; Zarzycki, P.; Banfield, J. F.; Gilbert, B. Mechanism of Ferric Oxalate Photolysis. *ACS Earth and Space Chemistry* **2017**, *1* (5), 270−276.

(16) Mulazzani, Q. G.; D'Angelantonio, M.; Venturi, M.; Hoffman, M. Z.; Rodgers, M. A. Interaction of formate and oxalate ions with

radiation-generated radicals in aqueous solution. Methylviologen as a mechanistic probe. *J. Phys. Chem.* **1986**, *90* (21), 5347−5352.
(17) Weller, C.; Horn, S.; Herrmann, H. Effects of Fe (III)-concentration, speciation, excitation-wavelength and light intensity on the quantum yield of iron (III)-oxalato complex photolysis. *J. Photochem. Photobiol., A* **2013**, *255*, 41−49.
(18) Rush, J. D.; Bielski, B. H. Pulse radiolytic studies of the reactions of HO2/O2 with Fe (II)/Fe (III) ions. The reactivity of HO2/O2 with ferric ions and its implication on the occurrence of the Haber-Weiss reaction. *J. Phys. Chem.* **1985**, *89* (23), 5062−5066.
(19) Sedlak, D. L.; Hoigné, J. The role of copper and oxalate in the redox cycling of iron in atmospheric waters. *Atmos. Environ., Part A* **1993**, *27* (14), 2173−2185.
(20) Wang, Z.; Xiao, D.; Liu, J. Diverse redox chemistry of photo/ferrioxalate system. *RSC Adv.* **2014**, *4* (84), 44654−44658.
(21) Jeong, J.; Yoon, J. pH effect on OH radical production in photo/ferrioxalate system. *Water Res.* **2005**, *39* (13), 2893−2900.
(22) Pozdnyakov, I. P.; Kel, O. V.; Plyusnin, V. F.; Grivin, V. P.; Bazhin, N. M. New insight into photochemistry of ferrioxalate. *J. Phys. Chem. A* **2008**, *112* (36), 8316−8322.
(23) Chen, J.; Zhang, H.; Tomov, I. V.; Rentzepis, P. M. Electron transfer mechanism and photochemistry of ferrioxalate induced by excitation in the charge transfer band. *Inorg. Chem.* **2008**, *47* (6), 2024−2032.
(24) Wang, Z.; Chen, C.; Ma, W.; Zhao, J. Photochemical coupling of iron redox reactions and transformation of low-molecular-weight organic matter. *J. Phys. Chem. Lett.* **2012**, *3* (15), 2044−2051.
(25) Zuo, Y.; Zhan, J. Effects of oxalate on Fe-catalyzed photooxidation of dissolved sulfur dioxide in atmospheric water. *Atmos. Environ.* **2005**, *39* (1), 27−37.
(26) Schauer, J. J.; Kleeman, M. J.; Cass, G. R.; Simoneit, B. R. Measurement of emissions from air pollution sources. 3. C1− C29 organic compounds from fireplace combustion of wood. *Environ. Sci. Technol.* **2001**, *35* (9), 1716−1728.
(27) Murov, S. L.; Carmichael, I.; Hug, G. L. *Handbook of Photochemistry*; CRC Press, 1993.
(28) Zuo, Y. *High-Performance Liquid Chromatography (HPLC): Principles, Procedures and Practices*; Nova Science: New York, 2014.
(29) Lavi, A.; Lin, P.; Bhaduri, B.; Carmieli, R.; Laskin, A.; Rudich, Y. Characterization of Light-Absorbing Oligomers from Reactions of Phenolic Compounds and Fe (III). *ACS Earth and Space Chemistry* **2017**, *1* (10), 637−646.
(30) Rodríguez, E.; Mimbrero, M.; Masa, F. J.; Beltrán, F. J. Homogeneous iron-catalyzed photochemical degradation of muconic acid in water. *Water Res.* **2007**, *41* (6), 1325−1333.
(31) Zhou, D.; Wu, F.; Deng, N.; Xiang, W. Photooxidation of bisphenol A (BPA) in water in the presence of ferric and carboxylate salts. *Water Res.* **2004**, *38* (19), 4107−4116.
(32) Zuo, Y. Light-induced formation of hydroxyl radicals in fog waters determined by an authentic fog constituent, hydroxymethanesulfonate. *Chemosphere* **2003**, *51* (3), 175−179.
(33) Liu, G.; Zheng, S.; Xing, X.; Li, Y.; Yin, D.; Ding, Y.; Pang, W. Fe (III)−oxalate complexes mediated photolysis of aqueous alkylphenol ethoxylates under simulated sunlight conditions. *Chemosphere* **2010**, *78* (4), 402−408.
(34) Zepp, R. G.; Hoigne, J.; Bader, H. Nitrate-induced photooxidation of trace organic chemicals in water. *Environ. Sci. Technol.* **1987**, *21* (5), 443−450.
(35) Jeong, J.; Yoon, J. Dual roles of CO2- for degrading synthetic organic chemicals in the photo/ferrioxalate system. *Water Res.* **2004**, *38* (16), 3531−3540.
(36) Zhao, C.; Arroyo-Mora, L. E.; DeCaprio, A. P.; Sharma, V. K.; Dionysiou, D. D.; O'Shea, K. E. Reductive and oxidative degradation of iopamidol, iodinated X-ray contrast media, by Fe (III)-oxalate under UV and visible light treatment. *Water Res.* **2014**, *67*, 144−153.
(37) Kozmér, Z.; Arany, E.; Alapi, T.; Takács, E.; Wojnárovits, L.; Dombi, A. Determination of the rate constant of hydroperoxyl radical reaction with phenol. *Radiat. Phys. Chem.* **2014**, *102*, 135−138.
(38) Herrmann, H.; Hoffmann, D.; Schaefer, T.; Bräuer, P.; Tilgner, A. Tropospheric aqueous-phase free-radical chemistry: Radical sources, spectra, reaction kinetics and prediction tools. *ChemPhysChem* **2010**, *11* (18), 3796−3822.
(39) Gligorovski, S.; Strekowski, R.; Barbati, S.; Vione, D. Environmental implications of hydroxyl radicals (· OH). *Chem. Rev.* **2015**, *115* (24), 13051−13092.
(40) Sandhiya, L.; Kolandaivel, P.; Senthilkumar, K. Mechanism and Kinetics of the Atmospheric Oxidative Degradation of Dimethylphenol Isomers Initiated by OH Radical. *J. Phys. Chem. A* **2013**, *117* (22), 4611−4626.
(41) Hoffmann, E. H.; Tilgner, A.; Wolke, R.; Böge, O.; Walter, A.; Herrmann, H. Oxidation of substituted aromatic hydrocarbons in the tropospheric aqueous phase: kinetic mechanism development and modelling. *Phys. Chem. Chem. Phys.* **2018**, *20* (16), 10960−10977.
(42) Yu, L.; Smith, J.; Laskin, A.; George, K. M.; Anastasio, C.; Laskin, J.; Dillner, A. M.; Zhang, Q. Molecular transformations of phenolic SOA during photochemical aging in the aqueous phase: competition among oligomerization, functionalization, and fragmentation. *Atmos. Chem. Phys.* **2016**, *16* (7), 4511−4527.
(43) Offenhauer, R. D. The direct esterification of phenols. *J. Chem. Educ.* **1964**, *41* (1), 39.
(44) Aihara, K.; Urano, Y.; Higuchi, T.; Hirobe, M. Mechanistic studies of selective catechol formation from o-methoxyphenols using a copper (II)−ascorbic acid−dioxygen system. *J. Chem. Soc., Perkin Trans. 2* **1993**, *2* (11), 2165−2170.
(45) Sun, Y.; Zhang, Q.; Anastasio, C.; Sun, J. Insights into secondary organic aerosol formed via aqueous-phase reactions of phenolic compounds based on high resolution mass spectrometry. *Atmos. Chem. Phys.* **2010**, *10* (10), 4809−4822.
(46) Steenken, S.; O'Neill, P. Oxidative demethoxylation of methoxylated phenols and hydroxybenzoic acids by the hydroxyl radical. An in situ electron spin resonance, conductometric pulse radiolysis and product analysis study. *J. Phys. Chem.* **1977**, *81* (6), 505−508.
(47) Atkinson, R.; Lloyd, A. C. Evaluation of kinetic and mechanistic data for modeling of photochemical smog. *J. Phys. Chem. Ref. Data* **1984**, *13* (2), 315−444.
(48) Glowacki, D. R.; Wang, L.; Pilling, M. J. Evidence of formation of bicyclic species in the early stages of atmospheric benzene oxidation. *J. Phys. Chem. A* **2009**, *113* (18), 5385−5396.
(49) Andino, J. M.; Smith, J. N.; Flagan, R. C.; Goddard, W. A.; Seinfeld, J. H. Mechanism of atmospheric photooxidation of aromatics: A theoretical study. *J. Phys. Chem.* **1996**, *100* (26), 10967−10980.
(50) Volkamer, R.; Platt, U.; Wirtz, K. Primary and secondary glyoxal formation from aromatics: experimental evidence for the bicycloalkyl- radical pathway from benzene, toluene, and p-xylene. *J. Phys. Chem. A* **2001**, *105* (33), 7865−7874.
(51) Wu, R.; Pan, S.; Li, Y.; Wang, L. Atmospheric oxidation mechanism of toluene. *J. Phys. Chem. A* **2014**, *118* (25), 4533−4547.
(52) Wang, L.; Wu, R.; Xu, C. Atmospheric oxidation mechanism of benzene. Fates of alkoxy radical intermediates and revised mechanism. *J. Phys. Chem. A* **2013**, *117* (51), 14163−14168.
(53) Zuo, Y.; Hoigné, J. Photochemical decomposition of oxalic, glyoxalic and pyruvic acid catalysed by iron in atmospheric waters. *Atmos. Environ.* **1994**, *28* (7), 1231−1239.

DOI: 10.1021/acs.est.8b04507
Environ. Sci. Technol. 2019, 53, 127−136